Technical Physics, 2025, Vol. 70, No. 3

13

# Study of PET substrate wetting by multicomponent graphene oxide suspensions

© A.V. Gushchin,[1] E.N. Dinkova,[1] L.A. Rayanova,[1] L.I. Salitrinnik,[1] M.I. Trukhanova,[2,3] I.A. Komarov[1,4]

[1] Moscow Polytechnic University,
107023 Moscow, Russia
[2] Lomonosov Moscow State University,
119991 Moscow, Russia
[3] Nuclear Safety Institute of the Russian Academy of Sciences,
115191 Moscow, Russia
[4] Federal Research Center for Problems of Chemical Physics and Medical Chemistry, Russian Academy of Sciences,
142432 Chernogolovka, Moscow region, Russia
e-mail: master_kom@mail.com

*Received November 22, 2024*
*Revised November 22, 2024*
*Accepted November 22, 2024*

The features of wetting of polymer PET substrates by multicomponent graphene oxide suspensions were studied. The possibility of improving the wetting of PET substrates by introducing additional organic components into commercially available graphene oxide suspensions was examined. N-Methylpyrrolidone, dimethylacetamide, and two types of enamel paint thinners were used as additional components. The wetting angle was reduced successfully in all cases. The drying time of droplets of multicomponent suspensions was also analyzed. Depending on the ratio of components and the type of dispersion medium, the drying time may vary by a factor of 3–40, which has a significant influence on the applicability of suspensions in aerosol deposition and centrifugation processes. The suspensions with n-methylpyrrolidone and dimethylacetamide remained stable for more than 2 months, and a stability period of approximately 1.5 months was demonstrated for the suspension with an enamel paint thinner.

**Keywords:** graphene oxide, dispersion medium, organic thinner, n-methylpyrrolidone, dimethylacetamide, PET substrate, wetting angle.

DOI: 10.61011/TP.2025.03.60865.406-24

## Introduction

Modern electronics advances not only in the „main“ direction of construction of increasingly fast and functional devices based on classical semiconductor materials, such as silicon, germanium, or $A^{III}B^{V}$ compounds, but also in the direction of fabrication of flexible [1] and organic [2] electronic devices. The trends in development of „smart“ electronic devices indicate that flexibility will become one of the most important requirements for such devices in the near future [3]. Flexibility should expand significantly the opportunities for integration of new devices. Specifically, it will become possible to produce flexible wearable solar panels, aircraft wings, car bodies, and other structures of complex non-rectangular shapes; chemical and biological sensors integratable into clothing; stents; implants; „smart“ tattoos; flexible displays, which are already being used in the latest generations of smartphones; etc. Recent world events have also clearly outlined the trend toward the construction of various drones, including bionic ones, that also require flexible materials (primarily for the fabrication of actuators [4]). In addition, since the reserves of indium on the Earth are limited, the search for alternative materials providing a low film resistance (on the order of several $\Omega/\square$) and high transparency (transmittance in the visible spectral region on the order of 85−90 %) is highly relevant. However, the above-mentioned tasks require novel materials that provide semiconductor (or simply conductive) properties coupled with mechanical flexibility.

The research into synthesis of new electronic materials potentially lifting the restrictions on flexibility and shape of electronic products has been ongoing since the 2000s. Various materials have been tested since the start of the 21st century. Among those attracting the most attention were carbon-based structures: fullerenes [5], nanotubes [6], graphene [7] and its derivatives (graphene oxide and reduced graphene oxide [8]), as well as organic semiconductors [9] and small organic molecules, which often feature semiconductor properties [10].

In addition, wearable devices are often fitted with a set of sensors, which currently includes an accelerometer, light sensor, barometer, and heart rate monitor. Wearable devices are a very promising platform for monitoring the health and environment of their user, and it is clear that the range of sensors integrated into them will expand significantly in the future. Specifically, the introduction of a set of chemical and biological sensors should help improve the quality of life of a person wearing such devices.

In the context of fabrication of chemical and biological sensors, reduced graphene oxide appears to be the most promising of all the mentioned materials. On the one hand, it provides flexibility, which is important for producing electrically conductive layers both in sensors and (potentially) in flexible solar panels and displays. On the other hand, various methods for controlling the degree of reduction of graphene oxide are already known [11,12]. Controlled reduction of graphene oxide should enable the construction of sensor electrodes and provide the broadest possibilities for its modification with various sensitive molecules.

Graphene oxide may be synthesized in different ways. The most common is the Hummers' method (both classical and modified). The production of graphene oxide by the Hummers' method involves the oxidation of graphite with a mixture of strong acids (sulfuric and nitric) in the presence of potassium permanganate. The obtained graphite oxide is subjected to ultrasonic treatment and rinsed with deionized water to remove residual acids and salts [13]. The resulting graphene oxide has a high concentration of oxygen-containing functional groups, which, in turn, makes it highly hydrophilic. Among the standout properties of graphene oxide obtained by the Hummers' method are the thickness of its sheets, which ranges from several nanometers to several micrometers, and strong absorption of light in the ultraviolet and visible spectral regions. It should also be noted that the electrical conductivity is initially low, but may still be adjusted by using certain thermal or chemical reduction methods and reducing the concentration of various functional groups [14,15].

The Staudenmaier method is fundamentally similar to the Hummers' one, but a mixture of nitric and sulfuric acid in the presence of potassium chlorate is used [16]. The yield of graphene oxide is increased due to the use of potassium chlorate that acts as a catalyst for the oxidation reaction. The primary disadvantage of the method is the production of chlorine gas in the reaction. Its advantages include the mentioned higher yield of graphene oxide and the potential for a more precise control (compared to the Hummers' method) over the degree of oxidation of graphene [17]. In addition, graphene oxide obtained this way is less prone to agglomeration in various dispersion media.

The Tour method is another acid-based synthesis technique [18]. A mixture of concentrated sulfuric and nitric acids is used in it, and several processing steps are added. In general, this method allows for even more precise control of the degree of graphene functionalization and the thickness and size of graphene oxide sheets [19]. In addition, graphene oxide obtained this way is even less prone to aggregation in various dispersion media.

The electrochemical synthesis of graphene oxide relies on exfoliation of graphite in the presence of an electrolyte [20]. Despite its simplicity, this method provides an opportunity to synthesize high-quality graphene oxide with a significant degree of graphitization. However, it requires specialized equipment and, consequently, is used less often than the three methods described above. Controlling the reaction conditions, such as electrolyte composition, pH, temperature, and applied voltage, one may achieve a high degree of homogeneity and low defect density of the synthesized graphene oxide sheets. In addition, the method allows for even more precise control over the degree of functionalization and the type of functional groups, opening up the possibility of synthesis of graphene oxide tailored for specific applications [21].

That said, controlled formation of uniform graphene oxide films of a given thickness on polymer substrates is still far from being a fully solved problem (especially in the context of at least small-scale industrial production). According to literature data, graphene oxide films may be formed in various ways. For example, the Langmuir–Blodgett method was used in [22,23]. On the one hand, this method allows one to form thin (even single-layer) films of graphene oxide; on the other hand, it has low potential for scalability and incurs long processing times for a single sample [24]. Drop-casting [25], dip-coating [26], and rod-casting [27] have also been used successfully to form graphene oxide films. However, these methods also have scalability issues and often fail to provide sufficient homogeneity of the applied film.

Aerosol deposition [28], inkjet printing [29], and spin-coating [30] deserve a mention among the methods that are best suited for synthesis of macroscale thin homogeneous films of graphene oxide. Aerosol deposition originated as a method that allows one to apply coatings to large-area surfaces. It is widely used in various industries and in the engineering of new materials and devices [31]. Just as aerosol deposition, inkjet printing belongs to the group of additive methods of formation of films and devices based on them and offers such advantages as high repeatability, scalability, and fairly high operating speed [32]. The main advantage of spin-coating is the rate and ease of synthesis of highly homogeneous films on the substrate surface [33].

All three of the above methods involve the use of solutions; therefore, the characteristics of interaction of the solution applied to the substrate are crucial for efficient film synthesis [32]. In all these three methods, the film formation process is affected significantly by the characteristics of the deposited solution (or, in the case of nanomaterials, the deposited suspension). One of the most important of them is wetting of the substrate by a suspension containing graphene oxide. Since water, which is the most common dispersion medium for graphene oxide, does not wet PET substrates well, one needs to increase the substrate surface wettability in one way or another. However, traditional methods of wettability enhancement (in particular, mechanical or plasma treatment [34]) may be inapplicable due to the formation of a significant relief of the substrate surface, which precludes one from synthesizing films with thicknesses on the order of a few nanometers. Another possibility is to alter the surface properties chemically by adding certain functional groups or molecules [35,36]. However, if applied in experiments with a graphene derivative, this approach is likely to affect the electronic properties of the resulting films, which is an undesirable effect.

Another approach is to modify wettability by adjusting the properties of the deposited graphene oxide-containing suspension itself. This requires the use of additional components that facilitate the dispersion of graphene oxide by themselves. Unfortunately, literature data on the features of dispersion of graphene and its derivatives in various dispersion media are scarce. A systematic description of approaches to selecting the optimum dispersion medium for graphene oxide has also not been compiled yet.

The authors of one of the earliest studies [37] examined the possibility of dispersing graphite oxide in 13 different dispersion media. It was demonstrated that, in addition to water (which was taken as a reference), graphene oxide may be dispersed in dimethylformamide, n-methylpyrrolidone, tetrahydrofuran, and ethylene glycol. The authors noted that the mechanisms for maintaining the stability in the above media remained unclear at the time of publication. A necessary but not sufficient prerequisite is a sufficiently high dipole moment of the dispersion medium, which allows for interaction with the functional groups contained in graphite or graphene oxide. However, the stability of a suspension in dimethyl sulfoxide, which has a significant dipole moment of 4.09 D, was weak.

An attempt to compare the dispersibility of graphene oxide in different media has also been made in [38], where nine organic solvents were examined as dispersion media (the tenth reference solvent was water). It was demonstrated that stable suspensions of graphene oxide form in tetrahydrofuran, dimethylformamide, ethylene glycol, and pyridine. In addition, the stability of suspensions based on water, dimethylformamide, ethylene glycol, and pyridine may be enhanced by introducing an additional suspension component: cholic acid (a surfactant). The use of mixed surfactants for stabilization of graphene suspension has been demonstrated later in [39].

The authors of [40] have tested the largest number of different organic solvents for dispersing graphene oxide and reduced graphene oxide. It was found that graphene oxide forms a stable suspension in such substances as n-methylpyrrolidone, dimethylformamide, and ethylene glycol, to which o-dichlorobenzene and 1-chloronaphthalene should be added in experiments on dispersing reduced graphene oxide. The authors cited the similarity of solubility parameters of the dispersion medium and the dispersed material (namely, the Hansen and Hildebrand parameters) as selection criteria. More specifically, the Hildebrand parameter ($\delta_T$) was used as the governing comparison criterion. Its values are $25.4\,\mathrm{MPa}^{1/2}$ and $22\,\mathrm{MPa}^{1/2}$ for graphene oxide and reduced graphene oxide, respectively, while the dispersion media have a Hildebrand parameter of $47.8\,\mathrm{MPa}^{1/2}$ (deionized water), $33\,\mathrm{MPa}^{1/2}$ (ethylene glycol), $24.9\,\mathrm{MPa}^{1/2}$ (dimethylformamide), and $23\,\mathrm{MPa}^{1/2}$ (n-methylpyrrolidone). Thus, according to the reported results, the dispersion medium should be selected by comparing its Hansen and Hildebrand parameters with those of graphene oxide or reduced graphene oxide.

The solubility of graphene oxide in various dispersion media has also been studied in [41]. The obtained results agreed in general with those discussed above. Tetrahydrofuran, n-methylpyrrolidone, dimethylformamide, and ethylene glycol are the solvents that form a stable dispersion medium for graphene oxide.

Reviewing the history of dispersion studies, one may note that a fairly small set of organic solvents potentially serving as a dispersion medium for graphene oxide has been investigated.

In the present study, we try to improve the wettability of PET substrates by using a multicomponent dispersion medium and evaluate the prospects of application of the examined multicomponent dispersion media in synthesis of graphene oxide films by aerosol deposition and spin-coating. One of the set criteria was that the additional component itself should be a fine dispersion medium for graphene oxide (or similar finely dispersed systems). N-Methylpyrrolidone ($\delta_T = 23\,\mathrm{MPa}^{1/2}$), which was found to provide stable suspensions of graphene oxide, was investigated as one of the additional components. Another component, which has previously been demonstrated to be suitable for dispersing functionalized carbon nanotubes (similar to graphene oxide in that they have a large number of different functional groups on their surface), was dimethylacetamide [42] with $\delta_T = 22.50\,\mathrm{MPa}^{1/2}$. It was also decided to examine a commercially available lacquer thinner, which is a mixture of ethylene glycol ($\delta_T = 33\,\mathrm{MPa}^{1/2}$), butyl glycol ($\delta_T = 20.8\,\mathrm{MPa}^{1/2}$), and methyl isobutyl ketone ($\delta_T = 17\,\mathrm{MPa}^{1/2}$), as an additional component of the dispersion medium. Generally speaking, such a mixture should ensure fine dispersibility of graphene oxide. A similar thinner with an added drying retarder was also tested. The indicated lacquer thinners are recommended for use in spray printing, where the sizes of dye particles are very close to those of graphene oxide particles.

It was found that all the mentioned additional components reduce the wetting angle of the multicomponent suspension (compared to the initial aqueous suspension), but provide significantly different droplet drying times. Thus, the lacquer thinner was identified as the optimum additional component, since the drying time determined in experiments with it is the closest to the characteristic time of spin-coating and aerosol deposition processes. At the same time, the multicomponent suspension with the lacquer thinner remained stable for at least 5 weeks without any additional ultrasonic treatment.

## 1. Materials and methods

An aqueous suspension of graphene oxide with a concentration of 3.11 mg/ml synthesized by the modified Hummers' method (OOO „MIP Grafen“, Russia) was used as the starting component for the preparation of multicomponent suspensions of graphene oxide. The

Ratio of components of multicomponent dispersions used in the study

| Ratio of components (initial GO dispersion: additional component) | Concentration of the obtained multicomponent dispersions, mg/ml |
|---|---|
| 1:9 | 0.31 |
| 2:8 | 0.62 |
| 3:7 | 0.93 |
| 4:6 | 1.24 |
| 5:5 | 1.56 |
| 6:4 | 1.87 |

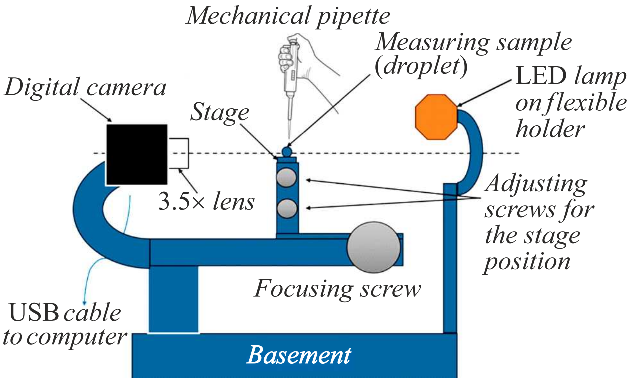

**Figure 1.** Diagram of the setup for wetting angle measurement.

characteristics of graphene oxide used in the present study were discussed in more detail in [43]. The additional components were n-methylpyrrolidone (N-MP; UHP, EKOS-1, Russia), dimethylacetamide (DMA; UHP, EKOS-1, Russia), a lacquer thinner (LT; Tamiya Ink., Japan), and a lacquer thinner with a retarder (LTr; Tamiya Ink., Japan). These components were mixed with the initial suspension in proportions listed in the table. Mixing was performed by sampling the required volume of the initial aqueous suspension of graphene oxide with a mechanical pipette and adding the required amount of the additional component of the dispersion medium (also with a mechanical pipette). The obtained multicomponent suspensions were then processed in a Stegler 10DT ultrasonic bath (240 W, China) for 30 min.

A PET film with a thickness of 125 $\mu$m and no additional surface treatment was used as a substrate for film deposition. Substrates $10 \times 10$ mm in size were used to determine the wetting angle. Prior to the wetting angle evaluation, the substrates were cleaned in 2-propanol with subsequent drying in an air flow with a pressure of 4 atm.

A proprietary instrument based on a UM-301 microscope was used to examine the wetting angle. It includes a horizontally mounted UM-301 microscope, a digital CMOS camera with a resolution of 5 MP (China), a PLAN $3.5 \times 0.10$ lens (LOMO, USSR), and a Levenhuk MS3 substage with a sample stage secured to it (Fig. 1). The substrate was secured to the sample stage with double-sided tape. Droplets were deposited manually using a mechanical pipette. Since a mechanical pipette was used, each measurement for each type of suspension was repeated at least 4 times to minimize dosing error. Wetting angle photographs were prepared using the software (ImageView) supplied with the digital camera. ImageView allows one to obtain photographs and video recordings (including those slowed down or sped up by a factor up to 20) through the microscope lens. The ImageJ program (https://imagej.net) was used to process data and determine the wetting angle. It is an open-source program developed by the US National Institutes of Health for analyzing and processing scientific images. The volume of droplets deposited by the mechanical pipette was 0.4 $\mu$l. The drying time was determined by identifying the moment of visual disappearance of a droplet viewed through the lens of the wetting angle meter and leveling of the PET substrate surface. This time was measured by the scale in the digital camera control program; the starting point was the moment a droplet hit the substrate, and the end point was the moment when liquid disappeared from the field of view . The images of droplets of multicomponent suspensions obtained using the software supplied with the camera were processed further with the „Contact Angle“ plugin in ImageJ.

The substrates were dried in a Stegler VAC-24 vacuum oven at a temperature of 110 °C for 30 min.

Raman spectra were recorded with an InVia spectrometer (Renishaw, UK) at a laser wavelength of 532 nm and an accumulation time at a point of 30 s (the overall spectrum measurement time was close to 20 min). High-magnification images of the surface were obtained using a Hitachi TM-3000 scanning electron microscope (Japan) at an accelerating voltage of 15 kV and a magnification of 1200×.

## 2. Results and discussion

The wetting angle and the drying time were determined by imaging a droplet with the digital camera of the wetting angle determination setup. Images of droplets of multicomponent suspensions of graphene oxide are presented in Fig. 2. The dependences of the wetting angle on the ratio of components of the dispersion medium were obtained for multicomponent suspensions of graphene oxide (Fig. 3). The dependences of the drying time of droplets of multicomponent suspensions on the ratio of components of the dispersion media were also obtained (Fig. 4). The dependence of the wetting angle on the concentration of graphene oxide in a multicomponent suspension was near-linear in all cases; the wetting angle increased with increasing concentration of graphene oxide. This general trend of the wetting angle increasing with concentration is characteristic of suspensions containing nanoparticles and was reported in [44,45]. The increase in wetting angle is attributable to the specifics of surface tension of a nanoparticle-containing liquid near the triple line,

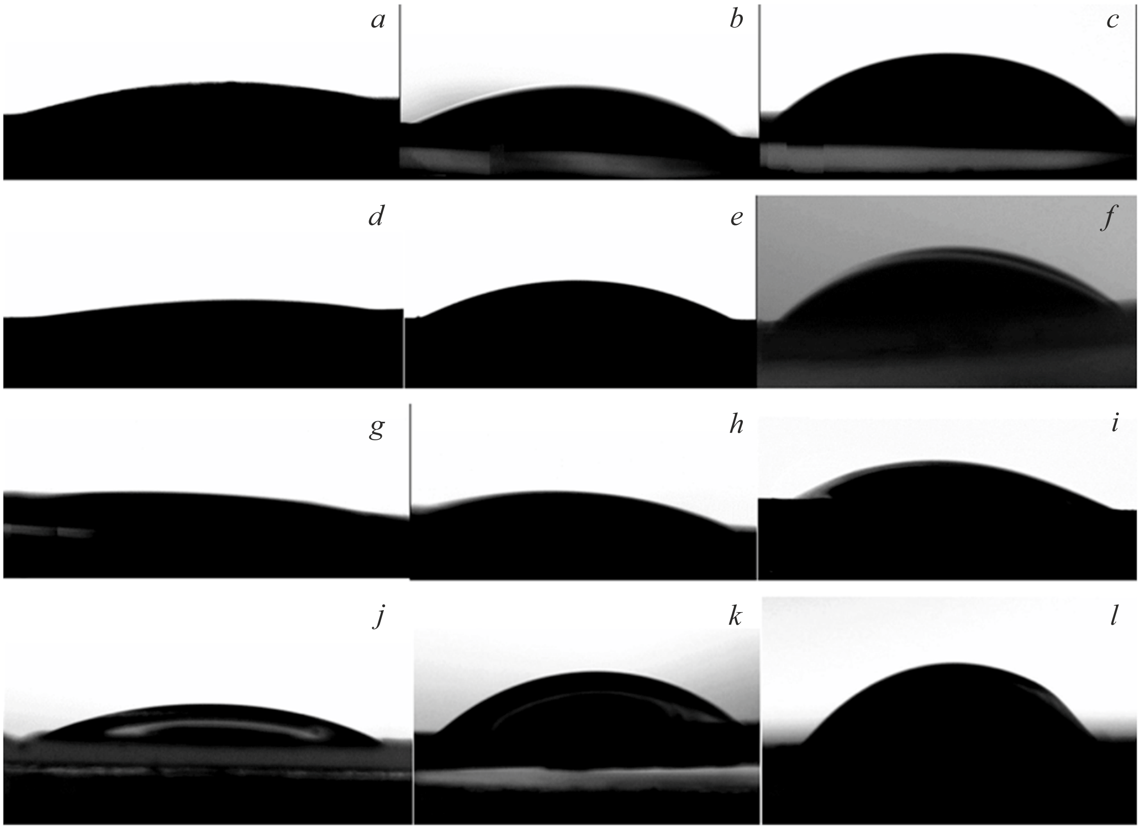

**Figure 2.** Photographic images of droplets of multicomponent GO dispersions with different (initial GO dispersion: additional component) ratios on a PET substrate: *a* — 1:9 in NMP; *b* — 3:7 in NMP; *c* — 6:4 in NMP; *d* — 1:9 in DMA; *e* — 3:7 in DMA; *f* — 6:4 in DMA; *g* — 1:9 in LT; *h* — 3:7 in LT; *i* — 6:4 in LT; *j* — 1:9 in LTr; *k* — 3:7 in LTr; and *l* — 6:4 in LTr.

which, in turn, changes due to the cohesive and adhesive interaction between water molecules and nanoparticles at the interphase surfaces, inducing an enhancement of the wetting angle at higher concentrations of nanoparticles. In certain cases (e.g., in a suspension of bismuth telluride nanoparticles), the wetting angle reaches its peak value at a specific concentration of nanoparticles [44].

In addition, according to [45], a reduction in particle size in the suspension leads to an increase in wetting angle, which is what is apparently observed in the present study, since the average wetting angle at high concentrations of NMP and DMA is 3–6° greater than the one corresponding to LT. It is assumed that a better dispersibility and a smaller size of graphene oxide particles are achieved in NMP and DMA, which is confirmed indirectly by the better stability of these suspensions observed during long-term (weeks and months) storage. It should also be noted that large values of the measurement error are attributable to the fact that the mechanical pipette was used for droplet deposition. Since this error cannot be eliminated in the current design of the setup, wetting angle measurements with droplets deposited onto separate substrates were repeated at least four times for each type of additional component and each concentration studied.

The obtained droplet drying times for suspensions containing NMP and DMA as additional components are rather significant and exceed 20 min (1200 s in Fig. 4 should be understood as „more than 1200 s“). Thus, judging by the drying time values, the suspensions containing LT or LTr as an additional component should be the best suited for film synthesis by spin-coating and aerosol deposition, since they provide drying times close to that of the indicated processes.

Apparently, the optimum medium for synthesis of thin films of graphene oxide on the surface of polymer substrates is a multicomponent suspension containing LT as an additional component with a concentration of 0.62–1.24 mg/ml, since the smallest spread in the wetting angle values is an indirect indication of the maximum homogeneity and stability of these dispersions.

On the one hand, the use of NMP and DMA as additional components of the dispersion medium is feasible; on the other hand, it will necessitate the use of a heating system for the substrate or the working chamber of the deposition setup and require a longer drying time after the deposition process. It should be noted that, apparently, DMA provides an opportunity to obtain a more stable dispersion medium, since the spread of wetting angle values is significantly smaller at all the studied concentrations of graphene oxide.

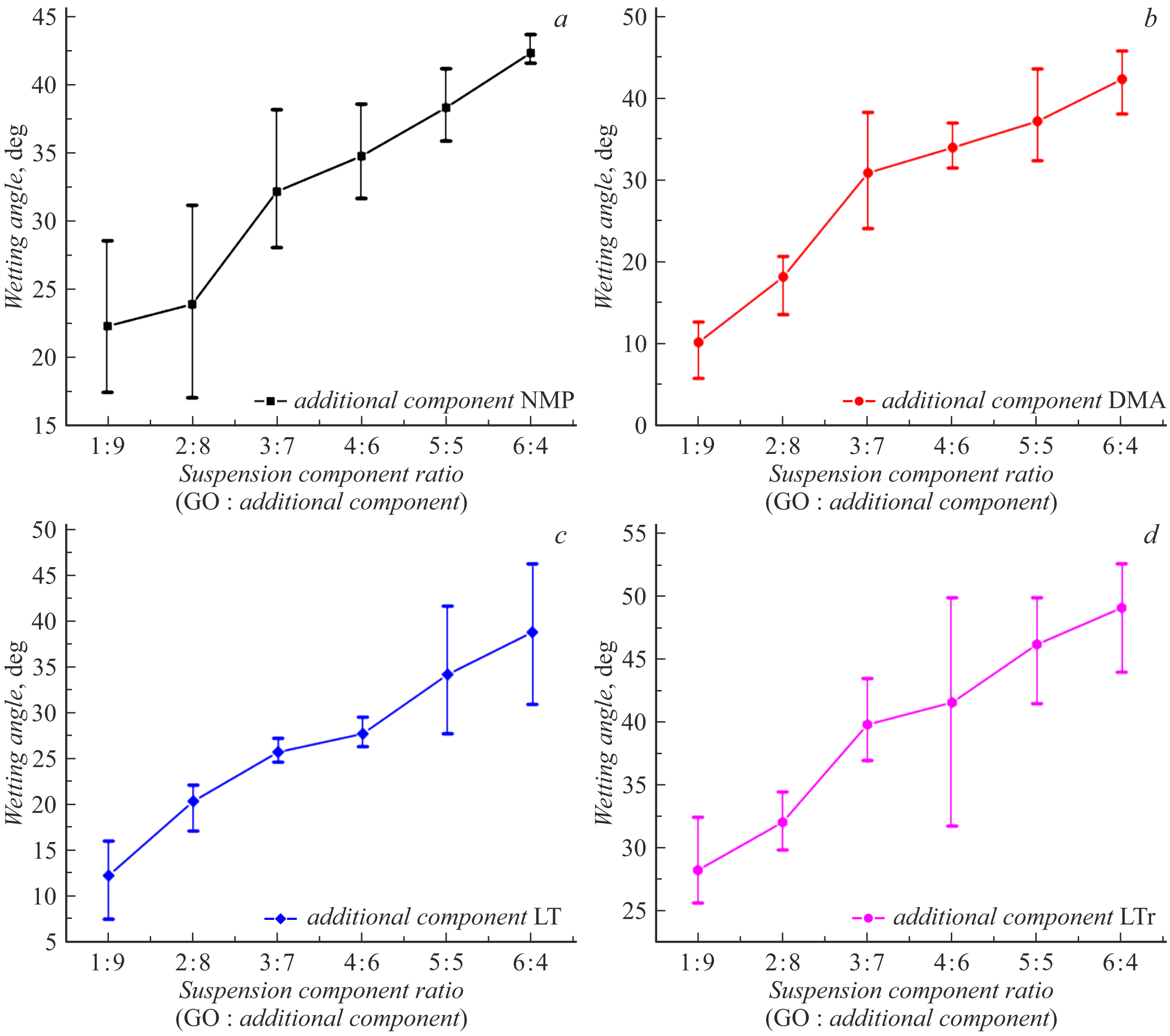

**Figure 3.** Dependence of the wetting angle on the ratio of dispersion components and the additional component type: NMP (*a*), DMA (*b*), LT (*c*), and LTr (*d*).

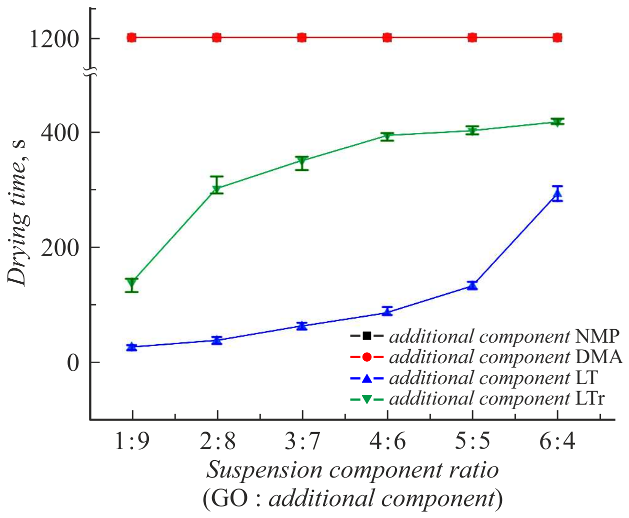

**Figure 4.** Dependence of the droplet drying time on the ratio of dispersion components and the type of additional component: NMP (*a*), DMA (*b*), LT (*c*), and LTr (*d*).

Thus, it was demonstrated that the use of additional components allows one to improve the wetting characteristics of PET substrates, and the most promising of these additional components is a lacquer thinner due to the similarity of the surface morphology of the resulting films and the fact that the drying time is close to the characteristic time of aerosol deposition and spin-coating processes. This should help reduce the overall time of film synthesis and avoid unnecessary complication of the deposition setup, since an additional heating chamber is not needed in this case.

Following droplet drying, the substrates were introduced into a vacuum oven and subjected to heat treatment at 110 °C for 30 min. The droplet regions were then imaged with a scanning electron microscope (SEM). Raman spectra of these regions were also measured.

SEM images of the PET surface with deposited droplets of multicomponent suspensions are shown in Fig. 5. It can be seen that only individual sheets of graphene oxide, which do not form a continuous film, are present in the

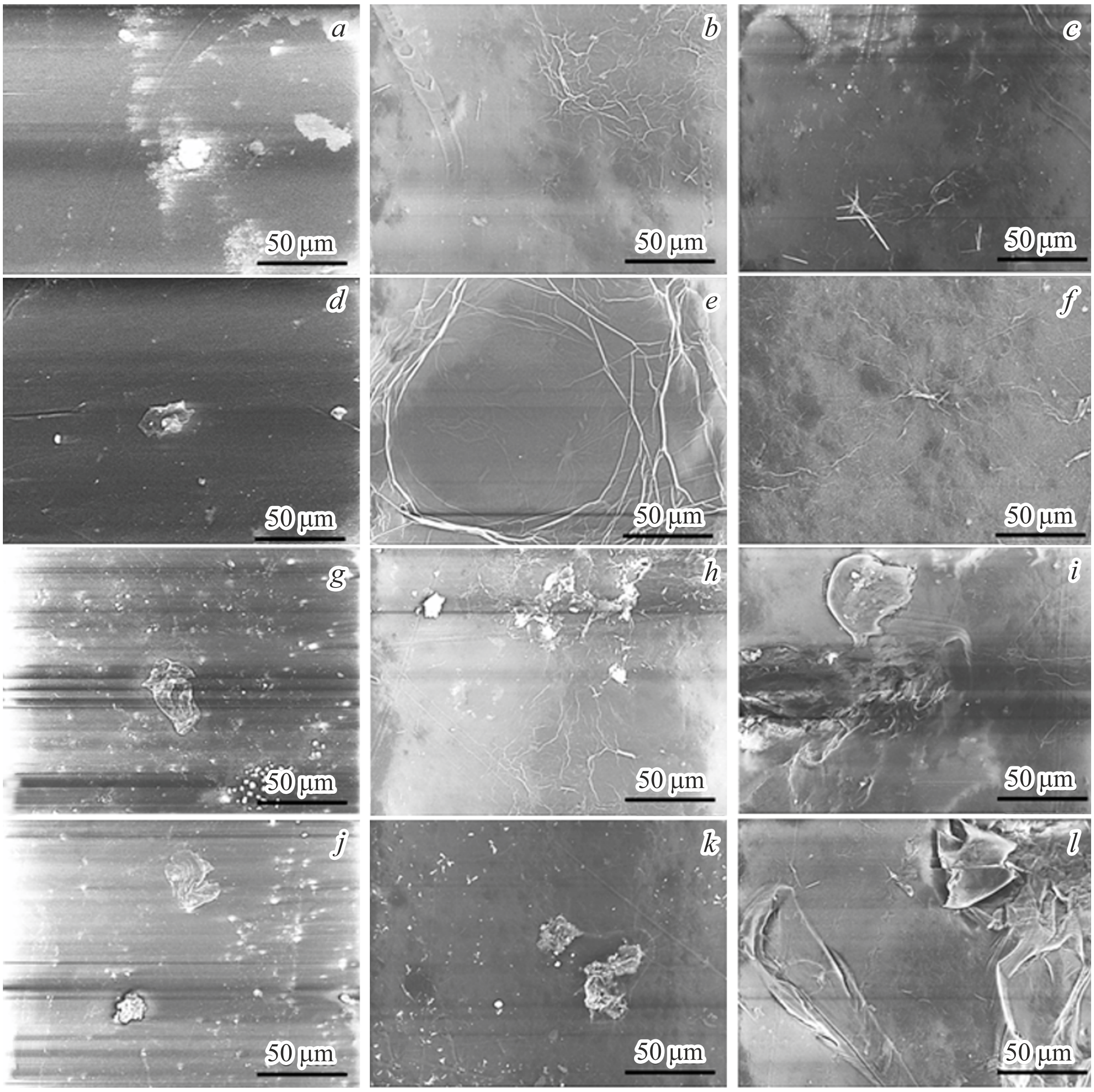

**Figure 5.** SEM images of GO dispersion droplets on the PET substrate: *a* — 1:9 in NMP; *b* — 3:7 in NMP; *c* — 6:4 in NMP; *d* — 1:9 in DMA; *e* — 3:7 in DMA; *f* — 6:4 in DMA; *g* — 1:9 in LT; *h* — 3:7 in LT; *i* — 6:4 in LT; *j* — 1:9 in LTr; *k* — 3:7 in LTr; and *l* — 6:4 in LTr.

region of a droplet of a suspension with a component ratio of 1:9 (a concentration of 0.31 mg/ml). Thus, regardless of the type of additional component used, minimum-concentration suspensions do not guarantee the formation of a continuous film. In view of this, suspensions of the indicated concentrations are applicable only in such cases where the deposition of loose individual sheets of graphene oxide is needed.

At higher concentrations of 3:7 and 4:6, a continuous graphene oxide film forms within a $50 \times 50\,\mu$m region. This is already useful for fabrication of chemical and biological sensors and flexible electronic devices. At even higher concentrations, a continuous film with less pronounced folding of the upper layer and a more significant difference in height is formed. These features are indicative of a substantial thickness of such films.

The results of Raman spectroscopy are consistent with the SEM imaging data: they reveal spectra typical of graphene oxide with characteristic peaks in the region of 1350, 1615, and 2950 $\mathrm{cm}^{-1}$. Figure 6 presents the dependence of the intensity ratio of peaks $D$, $G$, and $2D$ on the ratio of components of the dispersion medium. First, it should be noted that the shape of the obtained spectra is close to the one reported in literature [46]. In addition, the intensity ratio of the main characteristic peaks of graphene oxide is also consistent with the available data. Specifically, a slight linear growth of $I_D/I_G$ with increasing graphene oxide concentration is observed. According to [46], ratio $I_D/I_G$ characterizes the degree of graphitization of graphene oxide and increases with an increase in the number of defects. In the present study, the increase in $I_D/I_G$ should be attributed to the formation of films of a larger area and thickness (with

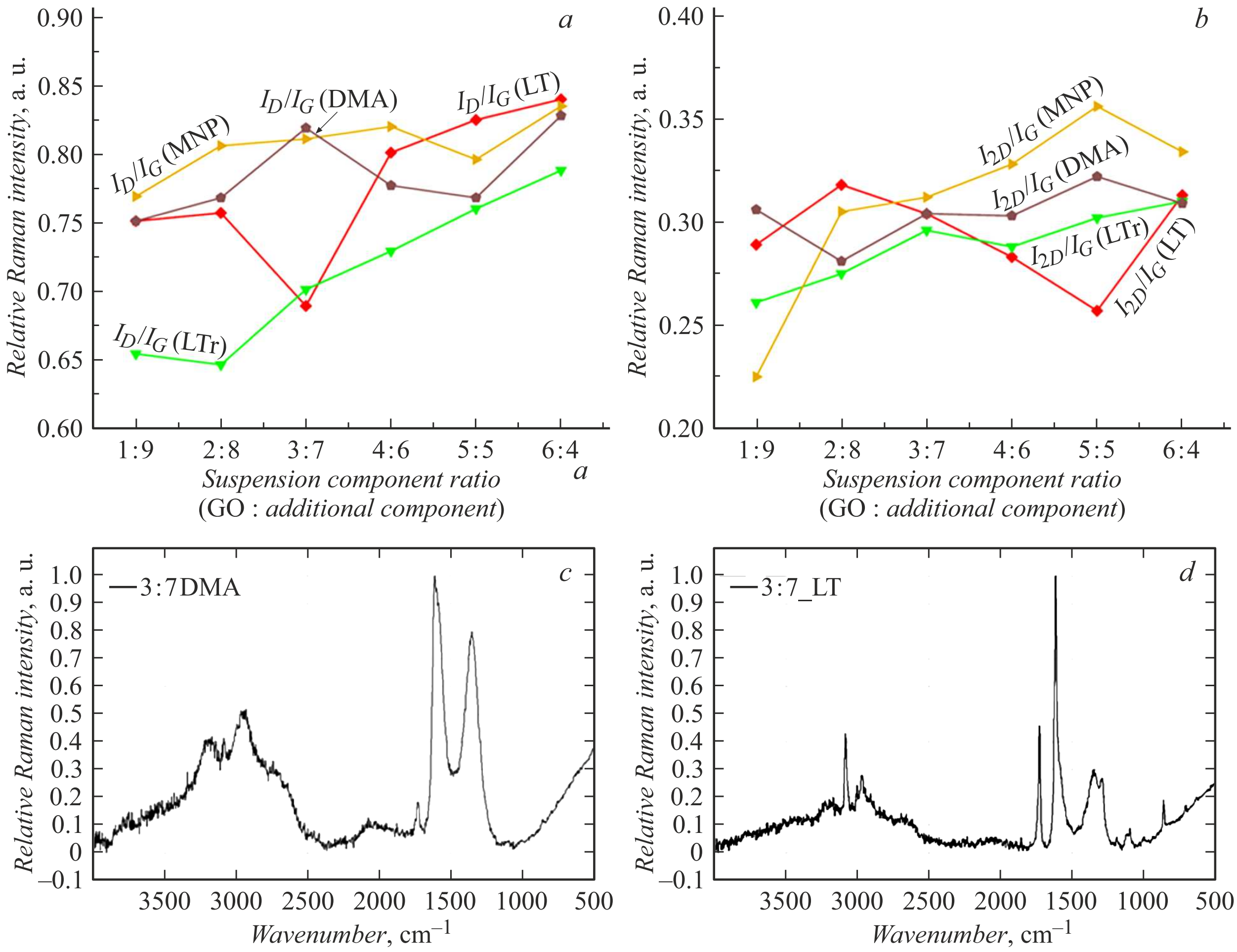

**Figure 6.** Dependence of the intensity ratio of peaks $I_D/I_G$ (*a*) and $I_{2D}/I_G$ (*b*) on the suspension component ratio; Raman spectra for a graphene oxide concentration of 0.92 mg/ml with DMA (*c*) and LT (*d*) being the additional component of the dispersion medium.

a corresponding increase in the amount of material from which the spectra are recorded). The $I_{2D}/I_G$ ratio remains unchanged within 0.05−0.1 a.u. in the case of deposition of graphene oxide films from suspensions containing NMP and LTr; in experiments with LT and DMA used as the additional components, this ratio fluctuates slightly around the values of 0.29 and 0.31, respectively. Therefore, it may be concluded that all the obtained films consist of separate sheets that are fairly close in thickness; i.e., all additional components provide similar levels of dispersion of the suspension. The formation of films of a larger area should be attributed to an increase in the concentration of graphene oxide; in the case of DMA and NMP, the thickness of films is greater than the one corresponding to LT and LTr, since peaks from PET are present in the Raman spectra in the latter two cases, indicating a smaller thickness of the deposited graphene oxide film. The obtained data on morphology and structure of graphene oxide films formed from multicomponent suspensions agree in general with literature data [47–49]. In addition, the lack of peaks unrelated to graphene oxide and PET in Raman spectra suggests that the dispersion medium is largely evaporated in the process of heat treatment at 150 °C in vacuum.

The stability of multicomponent suspensions was investigated by their visual examination for the presence of large agglomerates of graphene oxide. No agglomerates formed in more than 60 days of observation of suspensions with NMP and DMA used as the additional components. In the case of LT, agglomerates formed approximately after 40−45 days, and agglomeration in the suspension with LTr occurred within a few hours, which is naturally related to the presence of a retarder in it. It should also be noted that, according to [50,51], the degree of functionalization of graphene oxide changes during long-term storage. Specifically, it was demonstrated in [50] that the number of epoxy functional groups decreases during long-term storage in an oxygen-containing atmosphere. Thus, in-depth studies should take into account the possible variation of the degree of functionalization of graphene oxide both in a suspension and in a film. Therefore, it may be assumed that the degree of functionalization of graphene oxide in the dispersions examined in the present study does also change. At the same time, since carboxyl functional groups are the ones most important for immobilization of the sensitive layer molecules in sensors, a reduction in the number of epoxy groups should not have a noticeable effect on the characteristics of sensors.

In general, the obtained result does also verify indirectly the validity of determination of the optimum dispersion medium for graphene oxide based on the Hildebrand parameter value, since it is evident that multicomponent suspensions containing components with a Hildebrand parameter close to that of graphene oxide (or higher) are more stable, meaning the lack of visible macro-sized aggregates in them.

## Conclusion

The feasibility of control over the wetting characteristics of PET substrates via the introduction of additional organic components into a commercially available aqueous suspension of graphene oxide was demonstrated. A lacquer thinner is the best of the considered additional components in terms of processibility and potential to synthesize macro-sized films. N-Methylpyrrolidone and dimethylacetamide are also viable additional components, since the films obtained with their use have a somewhat lower defect density. However, a heating system for the substrate or the working chamber of the deposition system is required in this case. According to the electron microscopy data, films with dimensions sufficient for use in flexible electronics and sensor devices are formed with a component ratio ranging from 2:8 to 4:6 ($\sim 0.6-1.3$ mg/ml) with respect to the concentration of graphene oxide. In addition, the validity of the concept of determining the optimum dispersion medium based on the Hildebrand parameter was confirmed indirectly.

### Funding

This study was supported financially by the Moscow Polytechnic University as part of the P.L. Kapitsa grant program.

### Conflict of interest

The authors declare that they have no conflict of interest.

## References

[1] L. Li, L. Han, H. Hu, R. Zhang. Mater. Adv., **4**, 726 (2023). DOI: 10.1039/D2MA00940D

[2] C.S. Buga, J.C. Viana. Adv. Mater. Technol., **6** (6), 2001016 (2021). DOI: 10.1002/admt.202001016

[3] A.K. Katiyar, A.T. Hoang, D. Xu, J. Hong, B.J. Kim, S. Ji, J.-H. Ahn. Chem. Rev., **124**, 318 (2024). DOI: 10.1021/acs.chemrev.3c00302

[4] Q. Song, Q. Zhao. Appl. Sci., **14**, 4279 (2024). DOI: 10.3390/app14104279

[5] A.J. Khan, M. Hanif, M.S. Javed, S. Hussain, Z. Liu. J. Mater. Sci.: Mater. Electron., **30**, 8568 (2019). DOI: 10.1007/s10854-019-01177-4

[6] I.V. Novikov, N.I. Raginov, D.V. Krasnikov, S.S. Zhukov, K.V. Zhivetev, A.V. Terentiev, D.A. Ilatovskii, A. Elakshar, E.M. Khabushev, A.K. Grebenko, S.A. Kuznetsov, S.D. Shandakov, B.P. Gorshunov, A.G. Nasibulin. Chem. Eng. J., **485**, 149733 (2024). DOI: 10.1016/j.cej.2024.149733

[7] Y. Chendake, H. Mhetre, S. Khatavkar, V. Mehtre, S. Namekar, V. Kaduskar, P. Chougule. *Graphene: A Promising Material for Flexible Electronic Devices. Recent Advances in Graphene Nanophotonics* (Springer Nature, 2023), p. 83–118. DOI: 10.1007/978-3-031-28942-2

[8] H. Chen, F. Zhuo, J. Zhou, Y. Liu, J. Zhang, S. Dong, X. Liu, A. Elmarakbi, H. Duan, Y. Fu. Chem. Eng. J., **464**, 142576 (2023). DOI: 10.1016/j.cej.2023.142576

[9] Q. Zhang, W. Hu, H. Sirringhaus, K. Müllen. Adv. Mater., Special Issue: Organic Semicond., **34** (22), 2108701 (2022). DOI: 10.1002/adma.202108701

[10] H. Zhang, G. Zhao, Y. Tong, Q. Tang, Y. Liu. Scientia Sinica Chim., **54**—,(4), 406 (2024). DOI: 10.1360/SSC-2024-0006

[11] K.A. Shiyanova, M.V. Gudkov, M.K. Rabchinskii, L.A. Sokura, D.Y. Stolyarova, M.V. Baidakova, D.P. Shashkin, A.D. Trofimuk, D.A. Smirnov, I.A. Komarov, V.A. Timofeeva, V.P. Melnikov. Nanomaterials, **11** (4), 915 (2021). DOI: 10.3390/nano11040915

[12] A. Rowley, Y. Stehle, L. Kilby, C. Bashant. J. Carbon Research, **9** (3), 74 (2023). DOI: 10.3390/c9030074

[13] X. Chen, Z. Qu, Z. Liu, G. Ren. ACS Omega, **7** (27), 23503 (2022). DOI: 10.1021/acsomega.2c01963

[14] M. Abdollahi, M. Doostmohammadi, A.Z. Moshfegh. Carbon, **126**, 30 (2018). DOI: 10.1016/j.carbon.2017.09.091

[15] N. Hu, J. Li, S. Zhao, L. Zhang, W. Xu, P.K. Chu. J. Mater. Sci., **49** (4), 1661 (2014). DOI: 10.1007/s10853-014-8270-0

[16] A.A. Moosa, M.S. Abed. Turk. J. Chem., **45** (3), 493 (2021). DOI: 10.3906/kim-2101-19

[17] Y.J. Kim, Y.H. Kahng, Y.-H. Hwang, S.M. Lee, S.-Y. Lee, H.-R. Lee, S.H. Lee, S.H. Nam, W.B. Kim, K. Lee. Mater. Res. Express, **3** (10), 105033 (2016). DOI: 10.1088/2053-1591/3/10/105033

[18] A. Jiříčková, O. Jankovský, Z. Sofer, D. Sedmidubský. Materials, **15** (3), 920 (2022). DOI: 10.3390/ma15030920

[19] T.F. Emiru, D.W. Ayele. Egypt. J. Basic Appl. Sci., **4** (1), 74 (2017). DOI: 10.1016/j.ejbas.2016.11.002

[20] F. Liu, C. Wang, X. Sui, M.A. Riaz, M. Xu, L. Wei, Y. Chen. Carbon Energy, **1** (2), 173 (2019). DOI: 10.1002/cey2.14.

[21] A. Loudiki, M. Matrouf, M. Azriouil, A. Farahi, S. Lahrich, M. Bakasse, M.A. El Mhammedi. Appl. Surf. Sci. Adv., **7**, 100195 (2022). DOI: 10.1016/j.apsadv.2021.100195

[22] V. Periasamy, M.M. Jaafar, K. Chandrasekaran, S. Talebi, F.L. Ng, S.M. Phang, G.G. Kumar, M. Iwamoto. Nanomaterials (Basel), **12** (5), 840 (2022). DOI: 10.3390/nano12050840

[23] A. Holm, C.J. Wrasman, K.-C. Kao, A.R. Riscoe, M. Cargnello, C.W. Frank. Langmuir, **34** (33), 9683 (2018). DOI: 10.1021/acs.langmuir.8b00777

[24] O.N. Oliveira Jr., L. Caseli, K. Ariga. Chem. Rev., **122** (6), 6459 (2022). DOI: 10.1021/acs.chemrev.1c00754

[25] J. Kim, S. Park, M. Choi, S. Kim, J. Heo, E. Yeom, S. Kim, H. Lee, S. Kim. Diamond and Related Mater., **139**, 110327 (2023). DOI: 10.1016/j.diamond.2023.110327

[26] N. Murugesan, S. Suresh, M. Kandasamy, S. Murugesan, N. Pugazhenthiran, V. Prasanna Venkatesh, B.K. Balachandar, S.K. Kumar, M.N.M. Ansari. Physica B: Condensed Matter., **669**, 415288 (2023). DOI: 10.1016/j.physb.2023.415288

[27] K. Zhou, C. Guo, F. Gan, J.H. Xin, H. Yu. J. Colloid Interface Sci., **640**, 261 (2023). DOI: 10.1016/j.jcis.2023.02.107

[28] N.S. Struchkov, E.V. Alexandrov, A.V. Romashkin, G.O. Silakov, M.K. Rabchinskii. Fullerenes, Nanotubes and Carbon Nanostructures, **28**, 214 (2020). DOI: 10.1080/1536383X.2019.1686623

[29] C. Wang, M.J. Park, D.H. Seo, H.K. Shon. Separation and Purification Technol., **254**, 117604 (2020). DOI: 10.1016/j.seppur.2020.117604

[30] S.-Y. Kim, H.-E. Gang, G.-T. Park, H.-B. Jeon, Y.G. Jeong. Results Phys., **24**, 104107 (2021). DOI: 10.1016/j.rinp.2021.104107

[31] X. Wang, R.A. Paredes Camacho, X. Xu, Y. Wang, Y. Qiang, H. Kungl, R.-A. Eichel, Y. Zhang, L. Lu. Nano Mater. Sci., **6** (1), 24 (2024). DOI: 10.1016/j.nanoms.2023.11.002

[32] A. Silvestri, A. Criado, F. Poletti, F. Wang, P. Fanjul-Bolado, M.B. González-García, C. García-Astrain, L.M. Liz-Marzán, X. Feng, C. Zanardi, M. Prato. Adv. Functional Mater., **32** (2), 2105028 (2022). DOI: 10.1002/adfm.202105028

[33] S. Guo, J. Chen, Y. Zhang, J. Liu. Nanomaterials, **11**, 2539 (2021). DOI: 10.3390/nano11102539

[34] N. Al-Azzam, A. Alazzam. PLoS ONE, **17** (6), e0269914 (2022). DOI: 10.1371/journal.pone.0269914

[35] A. Cammarano, G. De Luca, E. Amendola. Cent. Eur. J. Chem., **11** (1), 35 (2013). DOI: 10.2478/s11532-012-0135-x

[36] S. Kim, R.A.R. Bowen, R.N. Zare. ACS Appl. Mater. Interfaces, **7**, 1925 (2015). DOI: 10.1021/am507606r

[37] J.I. Paredes, S. Villar-Rodil, A. Martinez-Alonso, J.M.D. Tascon. Langmuir, **24**, 10560 (2008). DOI: 10.1021/la801744a

[38] M.S. Khan, A. Shakoor, G.T. Khan, S. Sultana A. Zia. J. Chem. Soc. Pak., **37** (01), 62 (2015).

[39] B.-B. Feng, Z.-H. Wang, W.-H. Suo, Yi. Wang, J.-C. Wen, Y.-F. Li, H.-L. Suo, M. Liu, L. Ma. Mater. Res. Express, **7**, 095009 (2020). DOI: 10.1088/2053-1591/abb2ca

[40] D. Konios, M.M. Stylianakis, E. Stratakis, E. Kymakis. J. Colloid Interface Sci., **430**, 108 (2014). DOI: 10.1016/j.jcis.2014.05.033

[41] D.W. Johnson, B.P. Dobson, K.S. Coleman. Current Opinion Colloid Interface Sci., **20**, 367 (2015). DOI: 10.1016/j.cocis.2015.11.004

[42] I.A. Komarov, E.N. Rubtsova, A.S. Lapashina, A.V. Golovin, I.I. Bobrinetskiy. Biomed. Eng., **51**, 377 (2018). DOI: 10.1007/s10527-018-9753-8

[43] F.D. Vasileva, A.N. Kapitonov, A.E. Tomskaya, S.A. Smagulova. J. Structural Chem., **59** (4), 823 (2018). DOI: 10.1134/s002247661804011x

[44] S. Vafaei, T. Borca-Tasciuc, M.Z. Podowski, A. Purkayastha, G. Ramanath, P.M. Ajayan. Nanotechnology, **17**, 2523 (2006). DOI: 10.1088/0957-4484/17/10/014

[45] J. Chinnam, D. Das, R. Vajjha, J. Satti. Interna. Commun. Heat Mass Transfer, **62**, 1 (2015). DOI: 10.1016/j.icheatmasstransfer.2014.12.009

[46] A.C. Sparavigna. *Graphene and Graphene Oxide* (*Raman Spectroscopy*) (ChemRxiv, 2024). DOI: 10.26434/chemrxiv-2024-86stv-v2

[47] V. Scardaci, G. Compagnini. Data in Brief, **38**, 107306 (2021). DOI: 10.1016/j.dib.2021.107306

[48] R. Muzyka, S. Drewniak, T. Pustelny, M. Chrubasik, G. Gryglewicz. Materials, **11** (7), 1050 (2018). DOI: 10.3390/ma11071050

[49] L. Qian, A.R. Thiruppathi, R. Elmahdy, J. Van der Zalm, A. Chen. Sensors, **20** (5), 1252 (2020). DOI: 10.3390/s20051252.

[50] C.K. Chua, M. Pumera. Small, **11** (11), 1266 (2015). DOI: 10.1002/smll.201400154

[51] G. Sádovská, P. Honcová, J. Morávková, I. Jirka, M. Vorokhta, R. Pilař, J. Rathouský, D. Kaucký, E. Mikysková, P. Sazama. Carbon, **206**, 211 (2023). DOI: 10.1016/j.carbon.2023.02.042

*Translated by D.Safin*